Appl. Phys. B 92, 145–152 (2008)
DOI: 10.1007/s00340-008-3076-5

Applied Physics B
Lasers and Optics

G. BERGER✉
M. DIETZ
N. BRAUCKMANN
C. DENZ

Associative data search in phase-encoded volume holographic storage systems

Institut für Angewandte Physik, Westfälische Wilhelms-Universität Münster, Corrensstraße 2–4, 48149 Münster, Germany

Received: 3 September 2007/Final version: 25 April 2008
Published online: 27 June 2008 •

ABSTRACT We present a technique that enables true associative data search in phase-encoded volume holographic storage systems. The technique overcomes crucial shortcomings related to the only two methods proposed for associative searches in phase-encoded systems so far. An additional interferometric readout during content addressing is utilized to ascertain the cross-correlations between an input information and all data pages that are recorded by superposition in one location of the storage media. We present experimental investigations and thoroughly discuss the reliability of the technique. Under realistic conditions the inevitable normalization procedure, used to determine absolute correlation values, as well as the probability of small correlation values crucially affect the capabilities of associative search in phase-encoded holographic storage systems.

PACS 42.30.-d; 42.40.Pa; 42.79.Hp

1 Introduction

Volume holographic data storage has a great potential to become the basis of the next generation of optical storage devices. It provides high storage densities and fast transfer rates with extremely short data access times [1, 2]. These attributes are achieved by means of parallel, two-dimensional input and readout of digital data and superposition of many holograms in one location of a storage medium. The latter is based on exploiting the Bragg condition [3], which inherently offers the opportunity for angular and wavelength multiplexing (e.g. [4–6]). Other superimposing techniques can be created by combination or variation of these basic methods and spatial multiplexing (e.g. [7, 8]). Phase-code multiplexing is a variant of angular multiplexing [9]. It enables multiplexing of holograms in one location without requiring moving components [10] and provides two orders of magnitude higher signal-to-noise ratio in comparison to pure angular multiplexing [11, 12]. In addition, its special characteristics facilitate optical arithmetic operations during readout [13, 14] and enable very effective address-based data encryption [15–17].

Volume holographic storage systems also allow content addressed readout. By correlating input information against previously multiplexed data pages in Fourier space, efficient parallel data search can be realized. So far content addressing has been demonstrated in systems based on angular or phase-code multiplexing [18–22]. The implementation of associative data search in phase-encoded systems is not straightforward, since naturally the desired information is only comprised in the phase pattern of the generated correlation signal. So far, two simple approaches for performing associative recall in phase-encoded storage systems have been introduced [21]. The goal of these methods is to point out the storage address of the data page that best matches the input information. It is their most severe shortcoming that they do not allow access all cross-correlation values, which, in comparison, would inherently be accessible in systems based on angular multiplexing. Moreover, in order to provide a reliable performance, it is suggested to constrain the sparseness of the data pages [22]. Although the previously introduced methods can provide a better performance under certain conditions than it is achievable in systems based on angular multiplexing, their ability for associative data searching in phase-encoded systems is rather limited [22].

In this article we introduce an approach that overcomes the shortcomings of the previously proposed methods. By means of an additional interferometric readout step the phases and amplitudes of correlation peaks are determined. Subsequently, computational analyses reveal the desired cross-correlation values. In the following we briefly recapitulate the principles of phase-code multiplexing, present the experimental setup (Sect. 2.1) and discuss content addressing in phase-encoded systems (Sect. 3). The approach used to accomplish phase-resolved associative data search is explained in Sect. 4. Its implementation and experimental results are presented in Sect. 5. Finally, in Sect. 6 the reliability and limits of the new technique are discussed.

2 Background

In order to record data, a signal wave (S) containing the data to be stored and a coherent reference beam (R) interfere in the storage medium. Data is imprinted onto the signal wave as a two-dimensional amplitude (or phase) pattern, called a data page. In contrast to angular multiplexing, all reference beams interfere simultaneously with the signal wave. In order to store several data pages in one location, the phases of the reference beams are specifically

✉ Fax: +49-251-8333513, E-mail: gberger@uni-muenster.de

altered between subsequent recordings. The set of phase shifts (Φ_n) used to record a particular data page (D_n) is called its phase-code or phase address. In the reconstruction process, the media is illuminated by the N reference beams while the appropriate phase-code ($\Phi_{n'}$) of the desired data page is adjusted. In this step actually all previously stored data pages are reconstructed, since they have been recorded by the same reference beams. However, having employed suitable phase-codes during the storage process, all parts of unaddressed pages interfere destructively. In this manner data pages can be recorded and reconstructed independently with minimal noise [11, 12]. Appropriate orthogonal phase-codes can, for example, be constructed by means of Hadamard matrices [10, 23]. Throughout the investigations and experiments presented in this article, the one-dimensional Hadamard transformation kernel has been utilized to compute appropriate binary phase-code sets.

2.1 *Experimental specifications*

The presented experimental results are obtained in a 90°-setup, as depicted in Fig. 1. The beam of an optically pumped semiconductor laser (OPSL) ($\lambda = 488$ nm, cw) is split into a reference and a signal beam. In the signal arm a transmissive twisted nematic liquid crystal display (TN LCD) with a resolution of 800×600 pixels (32 μm pitch, 85% fill factor) is used to imprint amplitude modulated data pages onto the beam. A data page displayed by the spatial light modulator is focused to a point ≈ 2 mm in front of the storage media using a telescope arrangement as sketched in Fig. 1 ($f_1 = 80$ mm, $f_2 = -50$ mm, $f_3 = 80$ mm). In the reference arm a diffractive optical element (DOE) splits the incident collimated laser beam into 128 discrete beams. These beams are then focused ($f_4 = 160$ mm) on a one-dimensional nematic LCD that allows one to individually adjust their phases. Each pixel of the phase modulator is 2 mm long and 97 μm wide. By means of another lens behind the modulator ($f_5 = 100$ mm) 128 collimated reference beams are generated ($D \approx 1.5$ mm) that interfere in their point of intersection inside the storage medium with the signal wave. In the presented experiments typically 16 data pages are multiplexed, which allows the grouping of the reference beams into 16 sets of 8 beams that are distributed over the whole aperture. Thereby, effective intensities variations of just ±2.3% are be provided, allowing one to reliably investigate the proposed search technique. The phase modulator allows one to control the relative phase shift of each reference beam with an accuracy of $\approx 1\%$. In the presented experiments iron doped lithium niobate ($LiNbO_3$:Fe) is employed as storage material ($5 \times 7 \times 7$ mm^3). Holograms are recorded using an incremental recording schedule. Recording data pages with a sparseness of 0.25, the configuration provides an $M/\# = 2.5$. During the reconstruction process CCD cameras detect either the reconstructed data pages (CCD 1) or the resulting correlation signals when performing content addressing (CCD 2). By use of 4×4 oversampling and sparse modulation coding the setup was adjusted in a way that the reconstructed data pages exhibited bit error rates of $\leq 10^{-3}$.

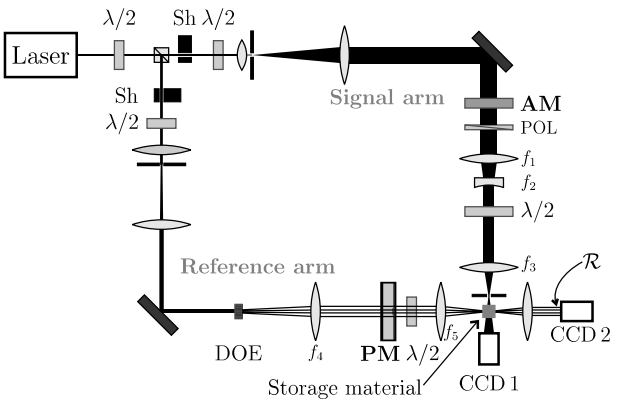

FIGURE 1 Volume holographic storage setup employing phase-code multiplexing. (AM = amplitude modulator; PM = phase modulator; DOE = diffractive optical element; λ/2 = half wave plate; Sh = shutter; POL = polarizer; CCD1 = camera for data page detection; CCD2 = camera for detection of correlation signals)

In terms of data searching, the goal is to find the addresses of the data pages that exhibit bit patterns that are highly congruent to the pattern presented as a search key. That is, a strong correlation signal should be produced if a search key and a recorded page possess ON pixels in the same positions. If compared pages significantly differ, only a weak signal should be produced. Therefore, a purely shift-invariant filtering operation is usually undesired, since it can give rise to misleading signals. In order to enable reliable data search the correlation operation should be space-variant. In volume holography horizontal shift-invariance practically does not occur due to the sharpness of the Bragg condition. However, in the Bragg degenerate direction vertical shift-invariance is typically present and may yield unintended signals [20]. In order to avoid misleading correlation signals it is appropriate to record in the Fresnel region [24]. As mentioned above, this is accomplished by focussing to a point ≈ 2 mm in front of the storage media. As a result, a linear space-variant filtering operation is enabled (in contrast to a "real" correlation) that allows pure optical bit-resolved comparison of any input information with all previously multiplexed data pages in parallel.

3 Content addressing in phase-encoded systems

During the recording process the Fresnel transforms $S_{1,\ldots,N}$ of the data pages $D_{1,\ldots,N}$ are recorded in the storage medium. The l-th signal wave and the corresponding reference wave can be written as

$$S_l = \hat{S}_l \mathrm{e}^{\mathrm{i}\boldsymbol{\sigma r}} \quad \text{and} \quad R_l = \sum_{m=1}^{N} R_m = \sum_{m=1}^{N} \hat{R} \mathrm{e}^{\mathrm{i}\boldsymbol{\varrho}_m \boldsymbol{r}} \mathrm{e}^{\mathrm{i}\phi_{lm}} . \tag{1}$$

The l-th reference wave consists of N separate reference beams, whose phases ϕ_{lm} are individually controlled. $\boldsymbol{\sigma}$ and $\boldsymbol{\varrho}_m$ are the wave vectors of the signal wave and of the m-th reference beam, respectively. $\hat{S}$ and $\hat{R}$ are the amplitudes of the waves, where $\hat{R}_m = \hat{R}$ has been assumed. After recording N data pages, the part of the refractive index modulation enabling content addressed readout is proportional to

$$\Delta n_{\mathrm{ass}} \propto \hat{S}^* \hat{R} \mathrm{e}^{-\mathrm{i}\boldsymbol{K r}} = \sum_{l=1}^{N} \sum_{m=1}^{N} \hat{S}_l^* \hat{R} \mathrm{e}^{\mathrm{i}\boldsymbol{K}_m \boldsymbol{r}} \mathrm{e}^{\mathrm{i}\phi_{lm}} , \tag{2}$$

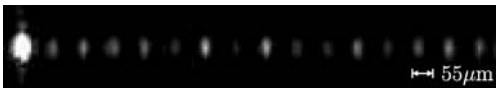

FIGURE 2 Content addressing of a stack of 16 multiplexed data pages. Magnified cutout of an experimentally obtained correlation signal (electronically enhanced using a logarithmic filter)

in which $\boldsymbol{K}_m = \boldsymbol{\varrho}_m - \boldsymbol{\sigma}$. The quantity $\hat{S}^*$ denotes the complex conjugate of $\hat{S}$. In order to perform associative search the storage media is addressed with a signal wave $S_\mathrm{a} = \hat{S}_\mathrm{a} \exp(\mathrm{i}\boldsymbol{\sigma r})$ bearing the data page D_a displayed by the amplitude modulator. Please note that throughout this article the index a denotes an addressing page. The output signal $\tilde{R}$ subsequently emerging from the storage media is given by the multiplication of S_a and (2). By means of a Fourier transform lens these reconstructed reference beams are focused, giving rise to a signal $|\mathcal{R}|^2$ picked up by the detector. The amplitude $\mathcal{R}$ can be written as [21]

$$\mathcal{R} = \mathcal{F}^{-1}\{\tilde{R}\} \propto \sum_{l=1}^{N}\sum_{m=1}^{N} \delta(x_m) * \left[\mathrm{e}^{\mathrm{i}\phi_{lm}} (D_l \star D_\mathrm{a})\right], \tag{3}$$

where $\star$ denotes the correlation operation. The indices n and m indicate page numbers and reference beam numbers, respectively. N denotes the total number of reference beams, which equals the number of data pages that can be multiplexed in one location by orthogonal phase-code multiplexing. The term $\exp(\phi_{l,(1,\ldots,N)})$ represents the phase-code used to record data page D_l. δ is the Kronecker delta and $\delta(x_l)$ corresponds to the Fourier transform of the l-th reference beam. The derivation of relation (3) is detailed in [21]. Equation (3) reveals that the search key is multiplied against all recorded data pages, producing optical cross-correlations $(D_m \star D_\mathrm{a})$. As emphasized above, the operation is not performed in Fourier space, but in the Fresnel region. Hence, according to [24], in this case the operation does not correspond to an exact correlation operation, but yields under ideal conditions the congruence of a recorded page D_m with an addressing page D_a in terms of matching ON pixels. Since each page has been recorded by means of all reference beams, each correlation gives rise to N reconstructed beams. All these correlations (of which each is composed by N beams) interfere and, eventually, N spatially separated correlations peaks appear at the positions x_m (in a row) in the back focal plane of the Fourier transform lens. An example of a correlation signal obtained with a CCD camera is shown in Fig. 2. A stack of 16 multiplexed data pages using phase-encoding is addressed by one of the recorded pages. Due to focussing by the FT lens, the dimensions of the correlation peaks are just a few pixels on the detector.

4 Phase-resolved data search

The goal of the parallel data search is to determine all cross-correlation values $c_{m\mathrm{a}} = (D_m \star D_\mathrm{a})$, simultaneously. Equation (3) indicates that each of the N correlation peaks $\mathcal{R}_n$ is composed by the sum of all correlation values $c_{m\mathrm{a}}$, taking the phases into account that have been adjusted during the recording process:

$$\mathcal{R}_l \propto \sum_{m=1}^{N} \mathrm{e}^{\mathrm{i}\phi_{lm}} c_{m\mathrm{a}}\,. \tag{4}$$

Splitting $\mathcal{R}_l$ into its amplitude $|\mathcal{R}_n|$ and phase φ_l, this can be written as

$$\alpha|\mathcal{R}_l|\mathrm{e}^{\mathrm{i}\varphi_l} = \sum_{m=1}^{N} h_{lm} c_{m\mathrm{a}}\,, \tag{5}$$

in which h_{lm} represents the elements of the employed Hadamard matrix. h_{lm} is either $+1$ or -1, according to phase shifts of 0 or π. Due to the use of binary phase-codes, the phase of each resulting correlation peak φ_l is also either 0 or π. In addition, in (5) a constant of proportionality, α, has been introduced, allowing one to replace the proportionality sign with an equals sign. In terms of the measured intensities of the correlation peaks (I_l) and the employed H-matrix used to generate the phase-codes, (5) can be rewritten as

$$H\boldsymbol{c} = \alpha \begin{bmatrix} \mathrm{e}^{\mathrm{i}\varphi_1}\sqrt{I_1} \\ \mathrm{e}^{\mathrm{i}\varphi_2}\sqrt{I_2} \\ \vdots \\ \mathrm{e}^{\mathrm{i}\varphi_N}\sqrt{I_N} \end{bmatrix} =: \alpha A_{1,\ldots,N}\,, \tag{6}$$

with $\boldsymbol{c} \equiv (c_{1\mathrm{a}}, c_{2\mathrm{a}}, \ldots, c_{N\mathrm{a}})^\mathrm{T}$. I_n corresponds to the measured intensity of the l-th correlation peak. That is, the quantity A_l denotes its amplitude, including its actual phase. The correlation values are determined by solving this equation for $\boldsymbol{c}$, which is straightforward when utilizing Hadamard matrices. Since H-matrices are orthogonal, $\mathrm{rank}(H) = \mathrm{rank}(H, \boldsymbol{c}) = N$ and $\det(H) \neq 0$ the Cramer rule can be applied and it follows:

$$\boldsymbol{c} = \alpha H^\mathrm{T} A_{1,\ldots,N}\,. \tag{7}$$

That is, in order to enable determination of the correlation values, the intensities and phases of the correlation peaks need to be measured. In addition, the normalization constant α has to be ascertained, if absolute correlation values are demanded.

5 Experimental implementation and results

The procedure of the phase-resolved data search can be divided into four steps. First, a stack of previously multiplexed holograms is addressed by a search key. If 16 pages have been recorded by means of phase-code multiplexing using Hadamard-related phase-codes, the resulting correlation signal is similar to that shown in Fig. 2. The first peak typically exhibits a very high intensity, whereas the intensity of any other peak is much lower. This characteristic is a result of the particular layout of Hadamard phase-codes. The phase of the first reference beam remains always unchanged, giving rise to solely constructive interference. The phase of every other reference beam is also often 0 or π, when recording a whole stack of data pages. During content addressing these parts interfere partly constructively and destructively typically yielding correlation peaks of much lower intensities. Hence, the employed camera should exhibit a large dynamic range in order to enable exact determination of the intensity

of each peak. If the dynamic range of the detector is not adequate, the demands can be significantly eased by recording just $N-1$ data pages. In this case it is sufficient to properly ascertain the intensities of $N-1$ peaks and the first peak can be omitted. This procedure may become more useful when multiplexing much more data pages. Though in this case the composition of correlation peaks is analogous, the contrast naturally increases.

In the second step the phases of all correlation peaks have to be determined. This can be accomplished by means of an additional interferometric readout. The superposition of the correlation signal with transmitted reference beams, whose phases and amplitudes are appropriately adjusted, suggests itself. As pointed out above, when utilizing H-matrices the phases of correlation peaks are either 0 or π. In this case the procedure is straightforward. Suppose the relative phases of the transmitted reference beams are adjusted to $\phi_{1,\ldots,N}=0$. That is, the first reference beam and the bright correlation peak interfere constructively and the intensity changes of all other peaks with respect to the pure correlation signal unambiguously reveal their phases.

In order to allow the determination of the absolute cross-correlation values in the third step, the measured intensities need to be normalized. The normalization can be accomplished by either method discussed below.

1. Inherent normalization
   One page with sparseness 1 (D_{ON}) is recorded among the actual data pages. It is assumed that the correlation between a search key and this page is equivalent to an autocorrelation signal, which is normalized to be 1 ($c_{\mathrm{ON_a}}=1$). Please note that, strictly speaking, this normalization is only correct for infinite SLM contrast, since in this case the OFF pixels do not contribute to the correlation signal. Against the background, when the modulator in our experiment provides a contrast of 580 : 1, the above assumption seems to be reasonable. Accordingly, assume that a white page is recorded by means of the first phase-code ($\phi_{1,(1,\ldots,N)}=0$). In this case $c_{1\mathrm{a}}=1$ and (7) yields

$$\alpha = 1\left(\sum_{l=1}^{N} \mathrm{e}^{\mathrm{i}\varphi_l}\sqrt{I_l}\right)^{-1}, \tag{8}$$

   which can subsequently be used to determine all other correlation values.
2. Separate normalization
   Another method for determining the constant α can be realized by electronically determining the correlation between the search key and an additional read out data page D_x. For instance, if the first page is read out and numerically correlated with the search key, the evaluation of(7) yields

$$\alpha = (D_x \star D_{\mathrm{a}})_{\mathrm{sep}}\left(\sum_{l=1}^{N} \mathrm{e}^{\mathrm{i}\varphi_l}\sqrt{I_l}\right)^{-1}. \tag{9}$$

   Figure 3b shows the normalized amplitudes, derived in the presented example, after separate normalization. In addition, the bar plot shows theoretical values that would be obtained in an ideal system.

Finally, the cross-correlation values can be computed according to (7). Figure 3c compares the experimentally obtained correlation values to the corresponding theoretical values. Although the absolute values slightly differ, the technique demonstrates its capability in determining an indexed list of recorded data pages sorted in terms of their congruence with the search key. In the examined example, an exact facsimile of the first page has been used as search information. The same procedure works, of course, if a search key is used that does not exactly match any of the recorded pages.

Various experiments are performed in order to quantitatively estimate the capability of the discussed data search technique and to compare the two normalization methods. All experiments are conducted under the same conditions. Table 1 summarizes the results in terms of the mean absolute errors and the standard deviation of the errors. It is apparent

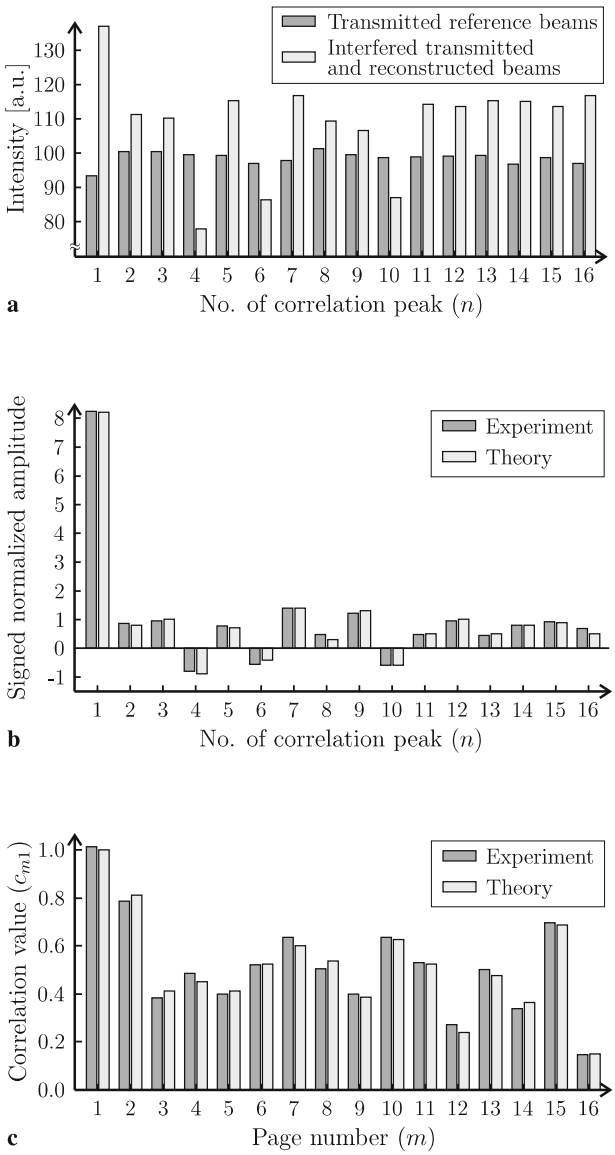

FIGURE 3 Associative data search with phase detection. Data page D_1 is used as search key $D_{\mathrm{a}}=D_1$. (**a**) Transmitted reference beams and interference signal of transmitted reference beams with correlation signal. (**b**) Signed normalized amplitudes. (**c**) Determined correlation values $c_{m\mathrm{a}}$

Addressing page	N	Normalization method	Mean absolute error	SD of the abs. errors
Exact copy of a recorded page	8	Inherent	3.3%	2.6%
		Separate	1.8%	0.6%
		Separate	2.3%*	1.8%*
Not recorded page	8	Inherent	3.2%	1.75%
		Separate	1.8%	0.65%
Exact copy of recorded page	16	Inherent	5.58%	4.9%
		Separate	4.4%	3.6%

*sparseness = 0.25

TABLE 1 Difference between theoretically and experimentally obtained correlation values for inherent and separate normalization (sparseness = 0.5; N = number of multiplexed pages; SD = standard deviation)

that in any situation separate normalization yields more accurate results. Recording a complete bright page, necessary for enabling inherent normalization, perturbs the homogeneity of the recorded holograms with respect to their diffraction efficiencies. Furthermore, the experimental practice has emphasized that a high dynamic range of the detector is necessary in order to exactly determine the intensities of all peaks simultaneously. This issue is also addressed in the following section.

6 Reliability of the phase-resolved data search

The impact of different noise sources on the reliability of the search technique is to be estimated. It is obvious that errors are dependent on the magnitude of unwanted amplitude and phase variations in the employed reference beams. Furthermore, it is a central question, whether amplitude variations in the signal arm, which are naturally present, have an impact on the expected error. Bearing the detailed discussion in [22] in mind, one should also consider the dependence of errors on the page sparseness. In order to provide absolute correlation values, the determined amplitude values have to be normalized. When employing the separate normalization procedure, it is a question of which page should be read out and numerically correlated with the search key in order to provide minimal errors. Finally, what are the error characteristics when multiplexing many data pages and does the finite dynamic range of the detector impose any constraints? In order to tackle all these questions, a computer simulation has been programmed that allows for independent control of all the indicated parameters. In all cases separate normalization is assumed.

The simulation starts by generating N random correlation values, where N is the number of data pages to be multiplexed. It is possible to limit the cross-correlations to certain values or to define maximal or minimal thresholds. Data pages and a search key are generated that obey the predefined correlation values. That is, assuming ideal conditions, addressing with the search key would exactly yield the predefined correlation values. Subsequently, the created data pages and the search key are distorted using amplitude filters that have been generated according to experimentally encountered unwanted intensity distributions of reconstructed pages. Thereby data pages are produced whose channel histograms (in terms of channel intensities) are extremely similar to histograms that are experimentally obtained. The search key is filtered by means of an amplitude mask that corresponds to that of a transmitted page in the storage system. The impact of these filters can be modified. The reference wave is composed of N beams, whose phases and amplitudes can individually be adjusted in the simulation. Prior to storage, the ideal amplitudes and phases are randomly distorted. The magnitude of phase and amplitude errors can independently defined. In the recording step all produced data pages are recorded using the distorted reference wave. Mathematically, in the simulation an $a \times b \times N$ matrix is produced that represents the stack of holograms usually recorded in the storage media. The matrix elements are typically complex numbers. $a \times b$ is the number of data channels per page. Using 4×4 oversampling in our configuration $a \times b = 30000$ channels. Each $(a \times b)_l$ submatrix corresponds to a mix of all data pages recorded by means of the l-th reference beam (with $i \in [1, 2, ..., N]$), taking the phases ϕ_{lm} into account (see Sect. 4). In order to investigate the associative data search, the whole matrix is addressed by the previously defined search key. Thereby cross-correlation amplitudes containing a phase are produced. Finally, corresponding correlation values are computed and compared with the ideal values by computing the mean absolute error (MAE). The whole simulation is repeated several times to allow reliable statistics. For each stack of different correlation values, different data pages and errors are generated. In the plots presented in the following sections each data point represents the average MAE found in the associative addressing attempts. Typically, each data point is determined by recording 2^{14} data pages. The error bars indicate the maximal and minimal mean errors. The simulation takes the grouping of reference beams into account (as discussed in Sect. 5), but neglects effects related to the dynamic range of the storage material.

6.1 *Impact of unwanted amplitude and phase variations*

Equation (7) emphasizes that the accuracy of determined correlation values depends on the homogeneity of the amplitudes of the reference beams and the preciseness of the modulated phase delays. Figure 4a shows the error characteristics when assuming ideal signal waves. In this simulation the number of multiplexed data pages have been assumed to be $N = 16$. It turns out that the mean error of the correlation values grows linearly with the magnitude of amplitude errors. The amplitude errors are produced by randomly distorting, i.e. attenuating or intensifying, the ideal reference wave. For a magnitude of the amplitude error that is equal to the one found in the realized system, the simulation emulates a mean correlation error of 3%. The total phase error considered in the graph constitutes of a random and a systematic error. The constant systemic error of 0.15% has empirically been found to enable a better description of actual experiments. The total phase error is varied from 0.4 up to 8%. As expected, the graph reveals that already moderate phase errors can severely deteriorate ascertained correlation values. However, based on the experimental specifications it becomes apparent that amplitude errors are the dominant error source related to the reference wave.

In order to investigate the impact of unwanted intensity variations in the signal arm, the filter used to deteriorate the

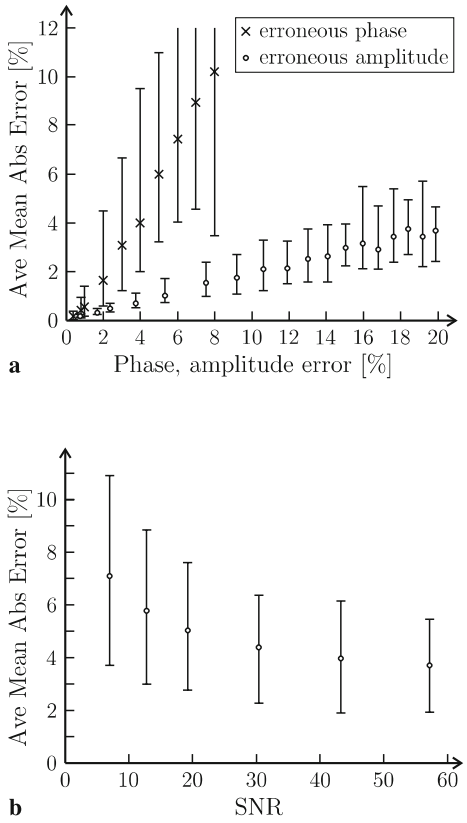

FIGURE 4 Mean absolute error (MAE) of correlation values. (**a**) MAE in the presence of solely phase or solely amplitude errors of the reference beams. (**b**) MAE vs. the signal-to-noise ratio of reconstructed data pages assuming an ideal reference wave

recorded data pages is varied. Basically, the distance and the width of the OFF and ON channel histograms are altered. The different filters can be distinguished in terms of the signal-to-noise ratio [25] related to data pages that are eventually reconstructed. In this simulation, ideal reference beams are assumed. Figure 4b shows the dependence of the average MAE on the signal-to-noise ratio (SNR). The mean error drastically increases when reducing the SNR. The effect is caused by a growing impact of non-zero OFF channels that contribute to the correlation peaks. The worse contrast of OFF and ON channels increasingly deteriorates the accuracy of the computed correlation values. Based on the specified attributes, the real phase-encoded storage system typically provides an SNR around 10. That is, under these conditions intensity variations in the signal arm are more critical than unwanted phase and amplitude variations related to the reference wave.

6.2 *Impact of the normalization procedure and the page sparseness*

It is obvious that the distortions caused by non-zero OFF channel amplitudes should also have an effect on the accuracy of the normalization process. Assume that separate normalization is used and that the reconstructed page is similar to the addressing page. In this case the numerically determined correlation value and the corresponding experimentally ascertained correlation value will be rather similar. On the other hand, as the cross-correlation decreases, the experimentally obtained correlation value gets more and more distorted due to a growing impact of the non-zero OFF channels. Hence, one expects that normalization should always be performed by means of the page that provides the highest similarity with the search key. The effect is investigated in Fig. 5, which shows the average MAE of determined correlation values versus the numerical cross-correlation of the search key and the page used for normalization. Below $c \approx 0.5$ the mean error considerably increases, emphasizing the relevance of picking an appropriate page for normalization. Experimentally, it is straightforward to identify the best matching page, since the relative correlation values are directly accessible after the first two readout steps.

Similarly, the sparseness of data pages should have an affect on the average error. In Fig. 6 the error characteristics are studied when decreasing the page sparseness in phase-encoded systems and in systems based on pure angular multiplexing. In this simulation it is assumed that the mean contrast of OFF and ON channels in reconstructed pages is around 10. In both configurations a decrease of the sparseness results in considerably growing errors. The graphs suggest that phase-encoding is advantageous. This effect is based on the different coding techniques. In an angular multiplexed system each data page is recorded by means of a single reference beam. Hence, during content addressing the strength of reconstructed reference beams directly indicate the congruence of a recorded page with a search key. In a phase-encoded system each data page is simultaneously recorded by N reference beams, where N is the total number of multiplexed pages. Each peak of a detected signal is composed by destructive and constructive interference of reconstructed reference beams that reflect cross-correlations of the search key with each of the recorded pages. That is, on average in this case, a lower sparseness and a non-zero OFF channel brightness are less critical. When increasing the number of multiplexed data pages and neglecting any other deterioration of holograms, this principle tends to decrease the dependence on the sparseness. However, the latter investigation has been performed under the assumption that intensity variations within the signal wave are small. Employing realistic variations as they have been encountered in our system, it turns out that the behavior shown in Fig. 6 can be considerably distorted, depending on the specific unwanted intensity distribution in the signal arm and the pattern of actually employed data pages.

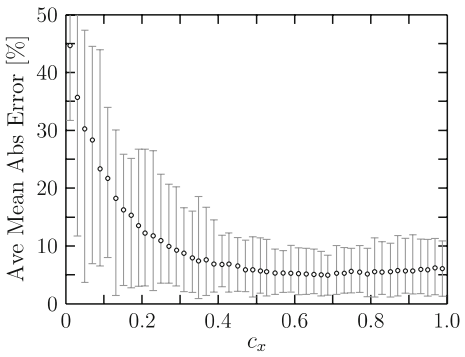

FIGURE 5 Error characteristics of correlation values derived during the associative data search. Effect of numerical normalization based on varying cross-correlations of the search key and a read out data page

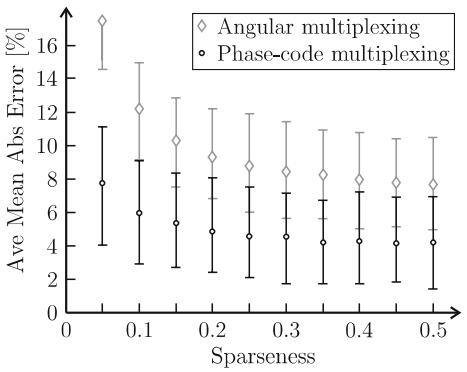

FIGURE 6 Dependence of the mean absolute error on the sparseness of recorded data pages

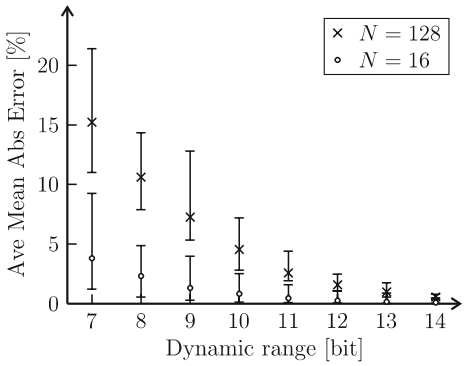

FIGURE 7 Dependence of the error characteristics of cross-correlation values on the dynamic range of the employed detector

As a result, the differences of associative search performed in systems based on angular or phase-code multiplexing with respect to the sparseness of data pages can become marginal.

6.3 *Further remarks*

In order to estimate the impact of phase and amplitude errors when increasing the number of multiplexed data pages, the simulation is run assuming the experimentally found error magnitudes. Omitting the effect of a limited dynamic range of the media, it turns out that the average MAE basically grows according to a sqrt-function in the range of $N \in \{2, 4, 8, ..., 128\}$. The effect is basically related to an increasing amplitude error of the reference beams, since the benefit of grouping beams successively decreases. The analysis emphasizes that neither the specified phase-errors nor the amplitude variations in the reference and signal arm are the cause of a significant deterioration of determined correlation values when increasing the number of multiplexed data pages. In a real system the dynamic range of the storage media, i.e. the corresponding quadratically decreasing diffraction efficiency, is suggested to be the most significant cause for a deterioration of ascertained absolute correlation values. Another problem arises due to the characteristics of Hadamard-related phase-codes. As mentioned in Sect. 5 the first correlation peak is typically very strong in comparison to other peaks. Nevertheless, all intensities need to be accurately detected. If all peaks are to be evaluated, a limited dynamic range of the employed camera can give rise to difficulties. The effect is investigated in Fig. 7 for $N = 16$ and 128. The contrast between the first and any other correlation peak typically increases, if more data pages are multiplexed. However, the graphs indicate that the error caused by the digitized detection becomes marginal above a dynamic range of approximately 12 bit. In this case the overall error is dominated by other error sources discussed above.

Eventually, the most important figure of merit for any data search method is the achievable search speed. In this context, it should be stated that the proposed technique is usually slower than the associative data search performed in systems based on pure angular multiplexing. This is mainly caused by the additional required readout step(s). Against this background, the time required to compute the correlation values based on the detected correlation peaks is negligible, since according to (7) the computation involves just $N \cdot N$ multiplications and $N \cdot (N-1)$ additions.

7 Conclusion

The presented technique is the first method that enables truly effective parallel search in phase-encoded volume holographic storage systems. This is accomplished by performing one (inherent normalization) or two (separate normalization) additional readout steps. The technique overcomes the shortcomings of any previously proposed search method for phase-encoded systems. It allows one to determine all cross-correlations between a search key and multiplexed data pages. As expected, any impreciseness with respect to the adjustment of relative phase shifts during recording processes have great impact on the search fidelity. A phase accuracy of $\approx 1\%$ does not give rise to any noteworthy constraint. With regard to the reference wave, it turns out that the inherent amplitude inhomogeneities (e.g. caused by the use of a DOE for beam preparation) have greater impact on the expected error characteristics. However, the numerical investigation reveals that the limited contrast of signal waves in real systems is likely to be the dominating error source. In order to guarantee reliable performance it is suggested to use a correlation peak detector that exhibits a dynamic range of at least 12 bit. This specification can be eased by skipping one phase code during the recording process.

ACKNOWLEDGEMENTS The authors would like to express their appreciation to G.W. Burr, IBM Almaden Research Center, for providing very helpful suggestions. The present work has been supported by the Hungarian Academy of Sciences, Project 436-UNG-113/165-01 and the Deutsche Forschungsgemeinschaft, Project 9160434.

REFERENCES

1 H.J. Coufal, D. Psaltis, G.T. Sincerbox (Eds.), *Holographic Data Storage*, (Springer, New York, 2000)
2 S.S. Orlov, W. Phillips, E. Bjornson, L. Hesselink, R. Okas, Proc. 29th Applied Imagery Pattern Recognition Workshop, Institute of Electrical and Electronics Engineers, New York (2000), pp. 71–77
3 E.N. Leith, A. Kozma, J. Upatnieks, J. Marks, N. Massey, Appl. Opt. **5**, 1303 (1966)
4 G.A. Rakuljic, V. Leyva, A. Yariv, Opt. Lett. **17**, 1471 (1992)
5 F.H. Mok, Opt. Lett. **18**, 915 (1993)
6 G.W. Burr, F.H. Mok, D. Psaltis, Opt. Commun. **117**, 49 (1995)

7 M.C. Bashaw, R.C. Singer, J.F. Heanue, L. Hesselink, Opt. Lett. **20**, 1916 (1995)
8 D. Psaltis, M. Levene, A. Pu, G. Barbastathis, K. Curtis, Opt. Lett. **20**, 782 (1995)
9 C. Denz, G. Pauliat, G. Roosen, T. Tschudi, Opt. Commun. **85**, 171 (1991)
10 C. Denz, G. Pauliat, G. Roosen, T. Tschudi, Appl. Opt. **31**, 5700 (1992)
11 K. Curtis, D. Psaltis, J. Opt. Soc. Am. A **10**, 2547 (1993)
12 M.C. Bashaw, J.F. Heanue, A. Aharoni, J.F. Walkup, L. Hesselink, J. Opt. Soc. Am. B **11**, 1820 (1994)
13 J.F. Heanue, M.C. Bashaw, L. Hesselink, Opt. Lett. **19**, 1079 (1994)
14 C. Denz, T. Dellwig, J. Lembcke, T. Tschudi, Opt. Lett. **21**, 278 (1996)
15 J.F. Heanue, M.C. Bashaw, L. Hesselink, Appl. Opt. **34**, 6012 (1995)
16 C. Denz, K.-O. Müller, F. Visinka, G. Berger, T. Tschudi, Proc. SPIE **4110**, 254 (2000)
17 G. Berger, K.-O. Müller, C. Denz, I. Földvári, Á. Péter, Proc. SPIE **4988**, 104 (2003)
18 P.A. Mitkas, G.A. Betzos, S. Mailis, A. Vainos, Proc. SPIE **3388**, 198 (1998)
19 G.W. Burr, S. Kobras, H. Hanssen, H. Coufal, Appl. Opt. **38**, 6779 (1999)
20 F. Grawert, S. Kobras, G.W. Burr, H.J. Coufal, H. Hanssen, M. Riedel, C.M. Jefferson, M.C. Jurich, Proc. SPIE **4109**, 177 (2000)
21 G. Berger, C. Denz, S.S. Orlov, B. Phillips, L. Hesselink, Appl. Phys. B **73**, 839 (2001)
22 G. Berger, M. Stumpe, M. Höhne, C. Denz, J. Opt. A Pure Appl. Opt. **7**, 567 (2005)
23 X. Yang, Z. Wen, Y. Xu, Proc. SPIE **2849**, 217 (1996)
24 M. Levene, G.J. Steckman, D. Psaltis, Appl. Opt. **38**, 394 (1999)
25 G.W. Burr, H. Coufal, R.K. Grygier, J.A. Hoffnagle, C.M. Jefferson, Opt. Lett. **23**, 289 (1998)